

Intermediate and ion-pair formation in the outer-sphere reactions between azido-pentacyanocobaltate(III) and iron(II) polypyridyl complexes in aqueous medium

Grace O. Ogunlusi · Jide Ige · Olayinka A. Oyetunji · Jonathan F. Ojo

Received: 7 January 2009 / Accepted: 8 April 2009 / Published online: 12 May 2009
© Springer Science+Business Media B.V. 2009

Abstract The kinetics of the reactions between azido-pentacyanocobaltate(III), $\text{Co}(\text{CN})_5\text{N}_3^{3-}$, and iron(II) polypyridyl complexes, $\text{Fe}(\text{LL})_3^{2+}$ (LL = bipy, phen), have been studied in both neutral and acidic aqueous solutions at $I = 0.1 \text{ mol dm}^{-3}$ NaCl. The reactions were carried out under pseudo-first-order conditions in which the concentration of $\text{Fe}(\text{LL})_3^{2+}$ was kept constant, and the second-order rate constants obtained for the reactions at 35 °C were within the range of 0.156–0.219 $\text{dm}^3 \text{ mol}^{-1} \text{ s}^{-1}$ for LL = bipy and 0.090–0.118 $\text{dm}^3 \text{ mol}^{-1} \text{ s}^{-1}$ for LL = phen. Activation parameters were measured for these systems. The dependence of reaction rates on acid was studied in the range $[\text{H}^+] = 0.001\text{--}0.008 \text{ mol dm}^{-3}$. The reaction in acid medium shows interesting kinetics. Two reactive species were identified in acid medium, namely, the protonated cobalt complex and the azido-bridged binuclear complex. The electron-transfer process is proposed to go by mixed outer- and inner-sphere mechanisms in acid medium, in which electron transfer through the bridged inner-sphere complex (k_5) is slower than through the outer-sphere path (k_4).

Electronic supplementary material The online version of this article (doi:10.1007/s11243-009-9220-1) contains supplementary material, which is available to authorized users.

G. O. Ogunlusi (✉) · J. Ige · J. F. Ojo
Department of Chemistry, Obafemi Awolowo University,
Ile-Ife, Nigeria
e-mail: roogunlusi2003@yahoo.co.uk

O. A. Oyetunji
Department of Chemistry, University of Botswana, Gaborone,
Botswana

Introduction

Electron-transfer reactions have been extensively studied due to their wide applications to different fields of chemistry [1–5]. In our earlier papers [6, 7], we reported the formation of ion-pairs in the reactions of $\text{Co}(\text{CN})_5\text{X}^{3-}$ (X = Cl, Br, I) with $\text{Fe}(\text{phen})_3^{2+}$ in aqueous acidic medium and the protonation of these halo-pentacyanocobaltate(III) complexes. So far, our investigations on the reactions of these halo-pentacyanocobaltate(III) complexes have presented very interesting results [6, 7] because of the relatively high protonation constants and ion-pairing constants of the cobalt complexes with the polypyridyl iron(II) complexes. The chemical reactions of the pentaamine complex, $\text{Co}(\text{NH}_3)_5\text{N}_3^{2+}$ [8, 9], have been extensively studied, but so far, studies on the analogous azido-pentacyanocobaltate(III) have been limited to crystallography, infrared and Raman spectra [10–12] and very scanty data have been reported on its chemical reactions [13, 14]. The redox partners $\text{Fe}(\text{LL})_3^{2+}$ and oxidant $\text{Co}(\text{CN})_5\text{N}_3^{3-}$ studied here are oppositely charged with a priori facilitation of ion-pair formation by electrostatic attraction. Here, we report the formation of a spectroscopically observable intermediate involving a bridging azide ligand. In addition, the protonation of the cobalt complex and the effects of ion-pair formation were studied. The ion-pair formation constants involved in the electron-transfer processes between the Fe(II) complexes and $\text{Co}(\text{CN})_5\text{N}_3^{3-}$ and the protonation constant of the cobalt complex have been determined.

Experimental

$\text{Fe}(\text{bipy})_3(\text{ClO}_4)_2$ and $\text{Fe}(\text{phen})_3(\text{ClO}_4)_2$ used were synthesised as reported earlier [15]. These complexes were

characterised by their UV/visible spectra. $\text{Fe}(\text{bipy})_3^{2+}$ showed maximum absorbance at 522 nm ($\epsilon = 8.58 \times 10^3 \text{ M}^{-1} \text{ cm}^{-1}$), while $\text{Fe}(\text{phen})_3^{2+}$ showed maximum absorbance at 510 nm ($\epsilon = 1.09 \times 10^4 \text{ M}^{-1} \text{ cm}^{-1}$). These values are in good agreement with those reported earlier [16]. $\text{K}_3\text{Co}(\text{CN})_5\text{N}_3$ was prepared from $[\text{Co}(\text{NH}_3)_5\text{N}_3]\text{Cl}_2$ using the method of Wilmarth [17]. $[\text{Co}(\text{CN})_5\text{N}_3]^{3-}$ gave a strong peak at 380 nm ($\epsilon = 600 \text{ M}^{-1} \text{ cm}^{-1}$). Elemental analysis for this complex was performed on a Vario EL Elemental analyzer. Anal.; Found: Co, 16.5; C, 16.9, N, 31.7; Calcd.; Co, 16.9; C, 17.2; N, 32.2; Co was determined using atomic absorption spectroscopy. These results show excellent agreement with calculated and literature values [18]. Hydrochloric acid (Riedel-deHaën) and Sodium chloride (BDH) were Analar grade.

All kinetic runs were performed under pseudo-first-order conditions with the concentration of the oxidant in large excess over that of the reductant. The kinetic data were obtained by monitoring the change in absorbance of the iron(II) complexes at λ_{max} 522 nm [for $\text{Fe}(\text{bipy})_3^{2+}$] and 510 nm [for $\text{Fe}(\text{phen})_3^{2+}$] using a Shimadzu UV-2501 PC spectrophotometer. The constant temperature for all kinetic runs was maintained within ± 0.1 °C in the cell compartment using a TCC 240A Peltier temperature controller. Cells of 1 cm path length were employed in all the studies. Deionised water was used for the preparation of all solutions. All reactions were monitored at 35.0 ± 0.1 °C except for the temperature dependence experiments. Ionic strength was maintained at 0.1 mol dm^{-3} using NaCl. Duplicate kinetic runs were carried out and the results agreed to within 5% precision.

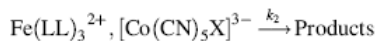
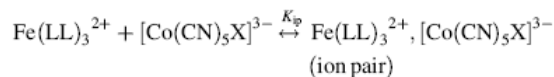
Results and discussion

The observed rate constants (k_{obs}) were obtained from the slope of plots of $\ln(A_t - A_\infty)$ against time. The plots were linear to more than four half lives with $R > 0.98$. Second-order rate constants were obtained by dividing k_{obs} by the concentration of Co(III) complex.

The effect of ionic strength on the reactions was investigated in neutral medium over the range $I = 0.005$ – $0.200 \text{ mol dm}^{-3}$ using NaCl. The results show a decrease

in the rate of reaction for both Fe(II) complexes as ionic strength increases. The temperature dependence was studied at 27.5, 32.0, 37.0, 40.0 and 45.0 °C. Plots of $\ln(k_2/T)$ against $1/T$ were linear ($y = -14,963x + 41.07$, $R^2 = 0.990$; $y = -14569x + 39.35$, $R^2 = 0.997$ for LL = bipy and phen, respectively) from which ΔH^\ddagger , and ΔS^\ddagger were obtained. ΔG^\ddagger was calculated from the values of ΔH^\ddagger and ΔS^\ddagger . Plots of $\ln k_2$ against $1/T$ which were also linear with negative slopes ($y = -15271x + 47.80$, $R^2 = 0.991$; $y = -14873x + 46.07$, $R^2 = 0.997$, for LL = bipy and phen respectively) from which E_a and A-factor values were calculated. The activation parameters calculated for these systems are shown in Table 1.

The variation in k_{obs} was investigated in neutral aqueous medium in the concentration range $[\text{Co}(\text{CN})_5\text{N}_3^{3-}] = 2.667 \times 10^{-3}$ – $1.00 \times 10^{-2} \text{ mol dm}^{-3}$ at fixed concentrations of iron(II) complex. k_{obs} was approximately constant at $[\text{Co}(\text{CN})_5\text{N}_3^{3-}] \geq 7.00 \times 10^{-3}$ and $8.667 \times 10^{-3} \text{ mol dm}^{-3}$ for the oxidation of $\text{Fe}(\text{bipy})_3^{2+}$ and $\text{Fe}(\text{phen})_3^{2+}$, respectively (Fig. 1). The stoichiometry was ascertained for each reaction from the amount of the reductant consumed, calculated from its peak absorbance, under the conditions of two- to threefold excess of the oxidant. Stoichiometry of both reactions (LL = bipy, phen) was found to be 1:1. The rate law for the reaction in neutral aqueous medium, corresponding to the mechanism



is given by

$$k_{\text{obs}} = \frac{k_2 K_{\text{ip}} [\text{Co}(\text{CN})_5\text{X}]^{3-}}{1 + K_{\text{ip}} [\text{Co}(\text{CN})_5\text{X}]^{3-}}$$

Plots of $1/k_{\text{obs}}$ versus $1/[\text{Co}(\text{CN})_5\text{N}_3^{3-}]$ were linear ($y = 4.0456x + 320.08$, $R^2 = 0.979$; $y = 7.9734x + 73.576$, $R^2 = 0.995$ for $\text{Fe}(\text{bipy})_3^{2+}$ and $\text{Fe}(\text{phen})_3^{2+}$). The K_{ip} values obtained from the slopes are 79.12 and 9.23 $\text{dm}^3 \text{ mol}^{-1}$ and k_2 values obtained from the intercepts are 0.0136 and 0.00312 $\text{dm}^3 \text{ mol}^{-1} \text{ s}^{-1}$ for the reactions of $\text{Co}(\text{CN})_5\text{N}_3^{3-}$ with $\text{Fe}(\text{bipy})_3^{2+}$ and $\text{Fe}(\text{phen})_3^{2+}$, respectively.

Table 1 Table of thermodynamic activation parameters and K_{ip} values

Redox system	ΔH^\ddagger (kJ mol ⁻¹)	ΔS^\ddagger (J mol ⁻¹ K ⁻¹)	ΔG^\ddagger (kJ mol ⁻¹)	E_a (kJ)	A	K_{ip} (dm ³ mol ⁻¹)
$\text{Fe}(\text{bipy})_3^{2+}/\text{Co}(\text{CN})_5\text{N}_3^{3-}$	+124.4 ± 1.7	+143.8 ± 1.3	+81.5 ± 0.5	126.9 ± 1.9	5.6×10^{20}	79.1
$\text{Fe}(\text{phen})_3^{2+}/\text{Co}(\text{CN})_5\text{N}_3^{3-}$	+121.0 ± 1.3	+129.3 ± 1.9	+82.5 ± 0.6	123.1 ± 1.1	1.0×10^{20}	9.2

$[\text{Fe}(\text{bipy})_3^{2+}] = 1.179 \times 10^{-5} \text{ mol dm}^{-3}$, $[\text{Fe}(\text{phen})_3^{2+}] = 1.00 \times 10^{-5} \text{ mol dm}^{-3}$, $I = 0.1 \text{ mol dm}^{-3}$, $[\text{Co}(\text{CN})_5\text{N}_3^{3-}] = 8.00 \times 10^{-3} \text{ mol dm}^{-3}$
Appropriate experimental data plots from which the parameters in this table were obtained are not shown but are available as supplementary data

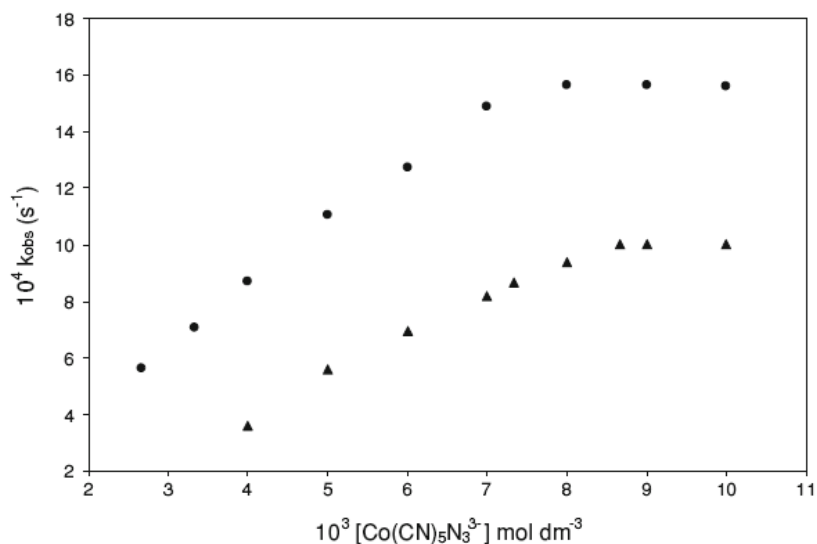


Fig. 1 Plot of k_{obs} against concentrations of $[\text{Co(CN)}_5\text{N}_3^{3-}]$. $[\text{Fe(bipy)}_3^{2+}] = 1.179 \times 10^{-5} \text{ mol dm}^{-3}$, $[\text{Fe(phen)}_3^{2+}] = 1.00 \times 10^{-5} \text{ mol dm}^{-3}$, $I = 0.1 \text{ mol dm}^{-3}$ $[\text{Co(CN)}_5\text{N}_3^{3-}] = 8.00 \times 10^{-3} \text{ mol dm}^{-3}$, filled circle Fe(bipy)_3^{2+} , filled triangle Fe(phen)_3^{2+}

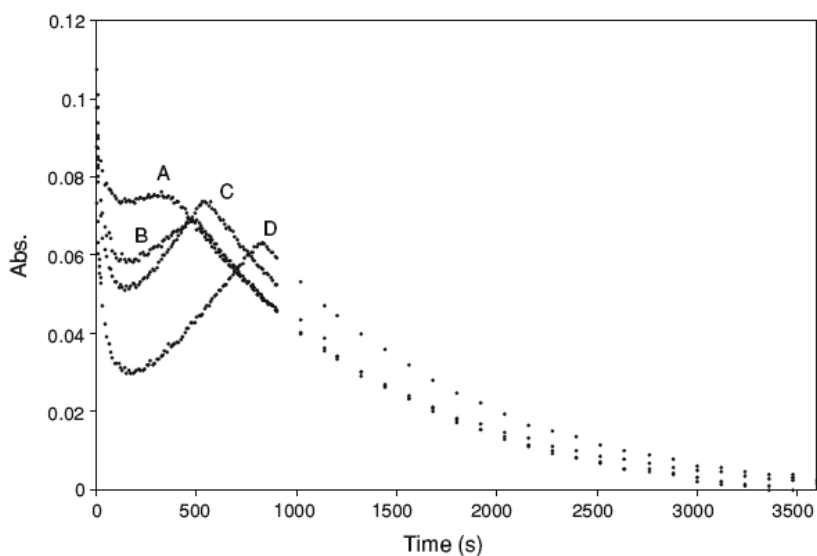


Fig. 2 Typical decay curves for the reaction of Fe(phen)_3^{2+} with $\text{Co(CN)}_5\text{N}_3^{3-}$ in the presence of acid, $[\text{Fe(phen)}_3^{2+}] = 1.00 \times 10^{-5} \text{ mol dm}^{-3}$, $I = 0.1 \text{ mol dm}^{-3}$ $[\text{Co(CN)}_5\text{N}_3^{3-}] = 8.00 \times 10^{-3} \text{ mol dm}^{-3}$, $T = 35.0 \text{ }^\circ\text{C}$; A: $[\text{H}^+] = 0.001 \text{ mol dm}^{-3}$, B: $[\text{H}^+] = 0.002$

mol dm^{-3} , C: $[\text{H}^+] = 0.004 \text{ mol dm}^{-3}$, D: $[\text{H}^+] = 0.008 \text{ mol dm}^{-3}$. Instrument was programmed to record absorbance every 2 s interval. Not all the data are shown here because of crowding

The reaction in aqueous acidic medium was investigated in the range $[\text{H}^+] = 0.001\text{--}0.008 \text{ mol dm}^{-3}$ using HCl while maintaining the ionic strength at 0.1 mol dm^{-3} with NaCl. The decay curves showed an initial decrease in

absorbance followed by an increase prior to electron transfer, in the final decay curve. This behaviour was not observed in neutral aqueous medium. The typical decay curves showing the formation and decomposition of the

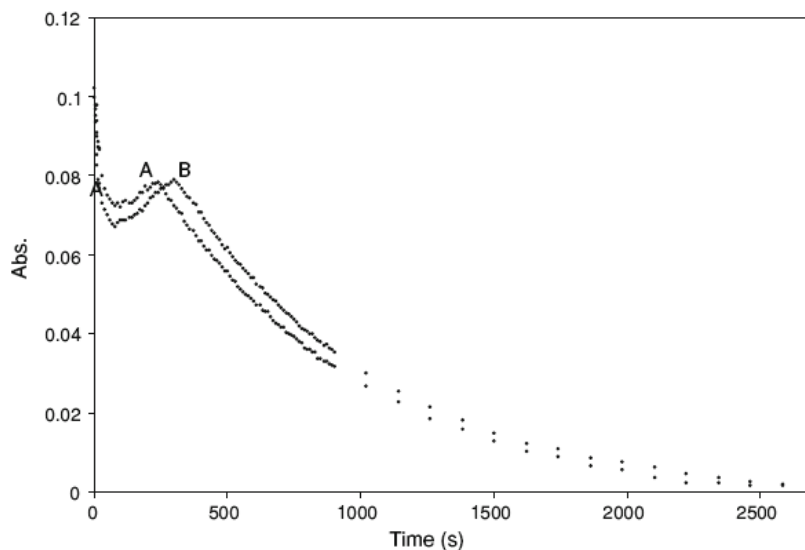
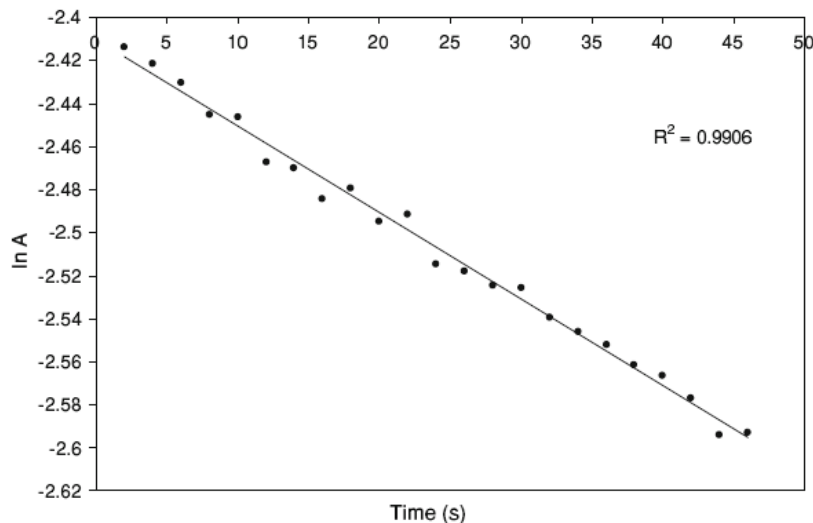


Fig. 3 Typical decay curves for the reaction of $\text{Fe}(\text{bipy})_3^{2+}$ with $\text{Co}(\text{CN})_5\text{N}_3^{3-}$ in the presence of acid, $[\text{Fe}(\text{phen})_3^{2+}] = 1.00 \times 10^{-5} \text{ mol dm}^{-3}$, $I = 0.1 \text{ mol dm}^{-3}$, $[\text{Co}(\text{CN})_5\text{N}_3^{3-}] = 8.00 \times 10^{-3} \text{ mol dm}^{-3}$, $T = 35.0 \text{ }^\circ\text{C}$; A: $[\text{H}^+] = 0.002 \text{ mol dm}^{-3}$, B: $[\text{H}^+] = 0.008 \text{ mol dm}^{-3}$. Instrument was programmed to record absorbance every 2 s interval. Not all the data are shown here because of crowding

Fig. 4 Typical plot of $\ln A$ against time for the initial decrease in the absorbance–time decay curve for the reactions of $\text{Fe}(\text{phen})_3^{2+}$ with $\text{Co}(\text{CN})_5\text{N}_3^{3-}$



intermediates are shown in Figs. 2 and 3. The specific rate constants for the observed three-stage process in the absorbance–time profiles were obtained using the method of initial rate. In order to avoid interferences from the various phases, data points at the onset of a new phase were not used. Not less than 20 data points were used for the first and the last phases. For the formation of the inner-sphere

phase, there were fewer data points because the phase is shorter in time. However, not less than 10 data points were used for this phase. The correlation coefficients for all absorbance–time plots were never less than 0.98. The graphs of $\ln A$ against time were linear with $R > 0.98$ (Fig. 4). The specific rate constants obtained are summarized in Table 2.

Table 2 Specific rate constants for the intermediate formation and electron-transfer process

[H ⁺] (mol dm ⁻³)	Fe(bipy) ₃ ²⁺			Fe(phen) ₃ ²⁺		
	k ₄ (dm ³ mol ⁻¹ s ⁻¹)	k _c (dm ³ mol ⁻¹ s ⁻¹)	10 ⁴ k ₅ (s ⁻¹)	k ₄ (dm ³ mol ⁻¹ s ⁻¹)	k _c (dm ³ mol ⁻¹ s ⁻¹)	10 ⁴ k ₅ (s ⁻¹)
0.001	0.225	0.075	1.560	0.338	0.038	1.098
0.002	0.563	0.100	1.486	0.838	0.075	1.205
0.004	0.675	0.163	1.560	1.075	0.138	1.153
0.008	1.000	0.187	1.542	1.638	0.163	1.125

Fe(bipy)₃²⁺ = 1.179 × 10⁻⁵ mol dm⁻³, [Fe(phen)₃²⁺] = 1.00 × 10⁻⁵ mol dm⁻³, I = 0.1 mol dm⁻³ [Co(CN)₅N₃³⁻] = 8.00 × 10⁻³ mol dm⁻³, T = 35.0 °C

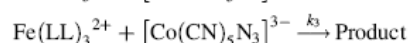
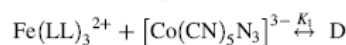
Discussion

Reaction in neutral aqueous medium

The saturation kinetics observed when k_{obs} was plotted against [Co(III)] suggests the formation of an ion-pair, non-bridging, transient precursor complex between the reactants prior to the electron-transfer process in neutral aqueous medium (Fig. 1). A non-bridging intermediate is expected from reactants that are inert to substitution. Ion-pair formation is facilitated by the opposite charges on the redox partners. These observations are also characteristic of an outer-sphere reaction mechanism. The ion-pair formation process is a necessary pre-equilibrium to give a reactive intermediate in the two redox systems studied. Plots of k_{obs} versus [oxidant] are similar to those obtained previously for the halopentacyanocobaltate(III) complexes [6]. Both Fe(II) complexes are known to be inert to substitution due to the non-availability of a co-ordination site for inner-sphere precursor complex formation. Outer-sphere mechanisms have been established for reactions of some polypyridyl-iron(II) complexes with Cr(IV) [19] and Co(III) [6, 20–22]. The first-order aquation rate constants obtained for Fe(phen)₃²⁺ and Fe(bipy)₃²⁺ at 35 °C are much smaller than the electron-transfer rate constants for their reactions with Co(CN)₅N₃³⁻ (i.e. $k_{\text{aq}} \ll k_{\text{et}}$). This observation together with linear plots [23, 24] of $1/k_{\text{obs}}$ versus $1/[\text{Co(CN)}_5\text{N}_3^{3-}]$ supports the postulate of an outer-sphere redox pathway. These profiles are also true for a mechanism involving the formation of a “dead-end” species as discussed below.

Electron-transfer rates for Fe(bipy)₃²⁺ reactions with the Co(III) complex are generally faster than those of Fe(phen)₃²⁺, as expected from free energy considerations, since Fe(bipy)₃²⁺ is a more powerful reductant considering their redox potentials. Ion-pair formation constants are affected by factors such as size of the anion and size of the complex ions [25]. Increase in the size of complex therefore results in decrease in the ion-pair formation constant. Variation of K_{ip} is due to the bulkier and more rigid Fe(phen)₃²⁺ compared to Fe(bipy)₃²⁺. The larger K_{ip} obtained for Fe(bipy)₃²⁺ shows that Fe(bipy)₃²⁺ is able to

approach the Co(III) center more closely due to reduced steric hindrance when compared with Fe(phen)₃²⁺. This enhances the transfer of an electron from Fe(bipy)₃²⁺ to Co(CN)₅N₃³⁻. This is also reflected in the larger A-value obtained for the reaction of Fe(bipy)₃²⁺ (Table 1). Relatively large ion-pair formation constants K_{ip} obtained for both reaction systems indicate the presence of strong electrostatic attraction between the oppositely charged reacting species, comparable with earlier results [20, 21]. The possibility of a “dead-end” mechanism can be excluded. For the reaction to follow a “dead-end” mechanism would require



where D is the dead-end adduct and

$$k_{\text{obs}} = \frac{k_3 [\text{Co(CN)}_5\text{N}_3^{3-}]}{1 + K_1 [\text{Co(CN)}_5\text{N}_3^{3-}]}$$

K_1 values calculated from this mechanism are identical with K_{ip} but k_3 values (0.125 and 0.247 dm³ mol⁻¹ s⁻¹) for the bimolecular electron transfer are much higher than k_2 (0.0136 and 0.00312 dm³ mol⁻¹ s⁻¹) for the intramolecular electron transfer within the ion pair. However, the nature of D is not chemically known or reasonable since both reactants are inert to substitution. Therefore, for chemical reasons, the ion-pair complex is preferred. The non-observation of an induction period within the response time of the equipment used is due to the spontaneous formation of the ion pair, as expected from the positive K_{ip} values.

The ionic strength dependence study for these redox systems shows a decrease in the rate of reaction as the concentration of NaCl increases, indicating that the reacting species carry opposite charges in the activated complex; $Z_A Z_B$ is therefore negative and increase in ionic strength will result in decrease in the rate of reaction. The addition of NaCl will necessarily reduce the electrostatic attraction and increase the distance of closest approach between the ion pair. This will in turn reduce the rate of electron transfer, in agreement with the experimental data.

The redox reactions were studied at different temperatures. Eyring's plot of $\ln(k_2/T)$ against $1/T$ (where k_2 is the specific rate constant for the intramolecular electron-transfer step within the ion-pair) was linear. The values of the A-factor and E_a were obtained from the corresponding Arrhenius plot. The results show that ΔH^* is positive for all the reactions, indicating that the activated complexes are endothermic. The large positive ΔS^* values imply that the activated complex is more disordered than the initial states of the reactants. Larger ΔS^* values for $\text{Fe}(\text{bipy})_3^{2+}$ can be explained by the flexibility of $\text{Fe}(\text{bipy})_3^{2+}$ in contrast to the more rigid $\text{Fe}(\text{phen})_3^{2+}$ forming a more disordered activated complex in the transition state of the former [26]. These reactions are kinetically and thermodynamically controlled. ΔG^* is essentially constant; the large ΔS^* values are compensated for by ΔH^* . The large values of A-factor obtained show the presence of a strong electrostatic force of attraction between the redox partners involved in the reactions. The thermodynamic parameters obtained are comparable to those reported earlier for the reactions of the halopentacyanocobaltate(III) complexes, which also proceeded through an outer-sphere mechanism [6].

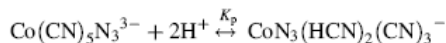
Reaction in aqueous acidic medium

The absorbance–time profile for reactions of the Fe(II) complexes with azido-pentacyanocobaltate(III) complex are triphasic (Figs. 2, 3). The observed minimum and maximum in these absorbance–time decay curves suggest two reactive species, assigned to the protonated cobalt

complex and the bridged binuclear complex as indicated in the reaction scheme below. Initially, we thought the intermediate species were a result of possible simultaneous protonation of the azido and cyano ligands of the azido-pentacyanocobaltate(III) complex before the electron-transfer process. Previous study by Staples [27] on some complexes of Co(III) and Rh(III) showed high ionization ratio for the protonation of azido complex of Rh(III). However, protonation rates are observed to be faster than the observed span of about 400 s in the present study. If the protonation time was up to 400 s, then it should be observable. Separate experiments carried out in the present study showed that protonation is indeed fast and not measurable by conventional techniques.

Investigation on the protonation of $\text{Co}(\text{CN})_5\text{N}_3^{3-}$ was carried out as previously reported [6, 28]. Typical spectroscopic evidence is shown in Fig. 5 for two acid concentrations. The full range of data which covered the concentration range $[\text{H}^+] = 0.00\text{--}0.10 \text{ mol dm}^{-3}$ is plotted in Fig. 6. The molar absorbance decreases with increase in the concentration of acid with complete protonation at $0.025 \text{ mol dm}^{-3}$ HCl.

The protonation step can be represented by:



The protonation constant K_p is given as

$$K_p = \frac{[\text{CoN}_3(\text{HCN})_2(\text{CN})_3^-]}{[\text{Co}(\text{CN})_5\text{N}_3^{3-}][\text{H}^+]^2}$$

As in previous study [6],

Fig. 5 UV–vis spectra of $\text{Co}(\text{CN})_5\text{N}_3^{3-}$ in the absence of acid and at two acid concentrations. A: no acid, B: $[\text{H}^+] = 0.006 \text{ mol dm}^{-3}$ and C: $[\text{H}^+] = 0.02 \text{ mol dm}^{-3}$

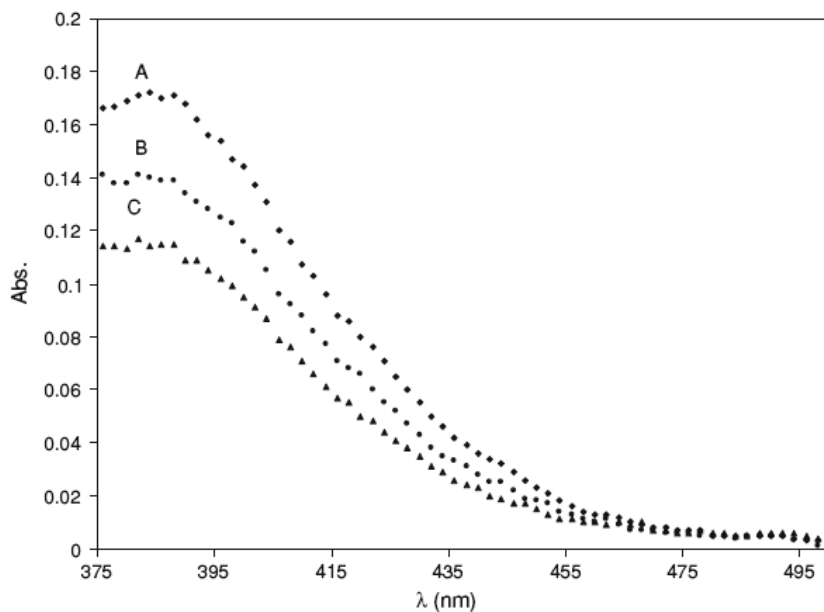
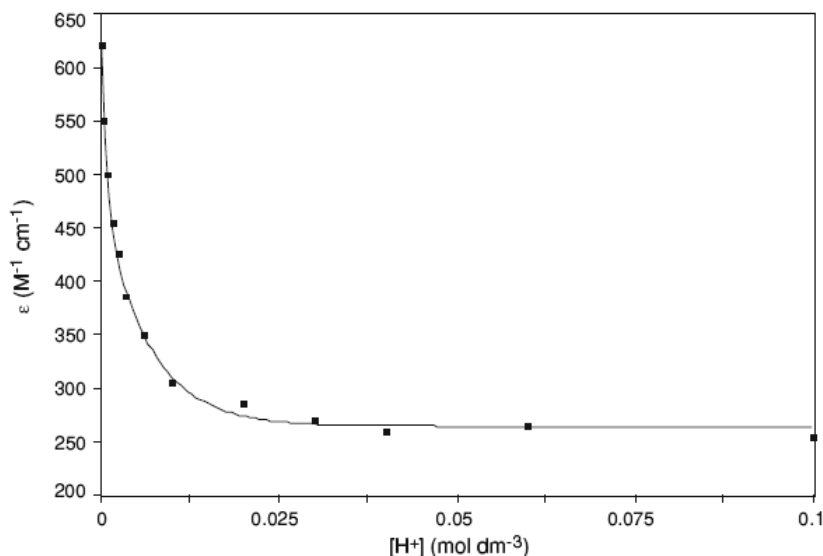


Fig. 6 Protonation curve showing the variation of the molar absorbances of $[\text{Co}(\text{CN})_5\text{N}_3]^{3-}$ with acid concentrations



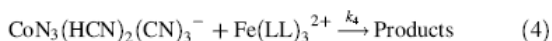
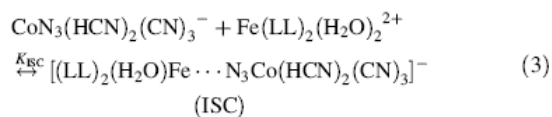
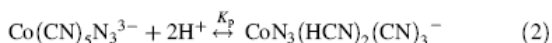
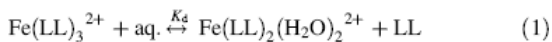
$$K_p = \frac{a_{pr}}{a_0 \times a^2}$$

and

$$a_{pr} = a_0 - \frac{A}{\varepsilon}$$

(where a , a_0 , and a_{pr} are the concentrations of acid, unprotonated complex and protonated complex, respectively. A = final absorbance of the unprotonated complex and ε = molar absorbance of the unprotonated complex). The protonation constant of $5.34 \times 10^2 \text{ mol}^2 \text{ dm}^6$ obtained for the two cyano ligands capable of protonation is within the range of those previously reported for the series $\text{Co}(\text{CN})_5\text{X}^{3-}$ which are 1.22×10^3 , 7.33×10^3 , and $9.90 \times 10^2 \text{ mol}^2 \text{ dm}^6$ for $\text{X} = \text{Cl}$, Br , and I , respectively, [6] confirming that the same cyano groups rather than the azido group were protonated.

The proposed mechanism for the reaction in acid medium is shown below:

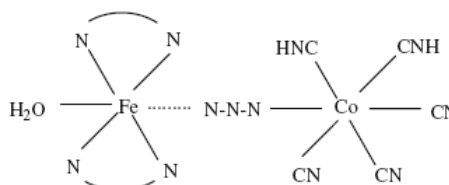


Overall rate is then given by

$$\begin{aligned} \text{Rate} &= k_4[\text{Co2H}][\text{Fe}(\text{LL})_3^{2+}] + k_5[\text{ISC}] \\ &= \frac{(k_4K_p[\text{LL}] + k_5K_{ISC}K_pK_d)[\text{Co}][\text{Fe}][\text{H}^+]^2}{[\text{LL}] + K_d + K_{ISC}K_pK_d[\text{Co}][\text{H}^+]^2} \end{aligned}$$

assuming equilibrium 3 to be far to the right and characterized by K_{ISC} , where $\text{LL} = \text{Phen}$ or bipy ; $\text{Co2H} = \text{CoN}_3(\text{HCN})_2(\text{CN})_3^-$; $\text{Co} = \text{Co}(\text{CN})_5\text{N}_3^{3-}$; $\text{Fe} = \text{Fe}(\text{phen})_3^{2+}$ or $\text{Fe}(\text{bipy})_3^{2+}$ and ISC (inner-sphere complex) = $[(\text{LL})_2(\text{H}_2\text{O})\text{Fe} \cdots \text{N}_3\text{Co}(\text{HCN})_2(\text{CN})_3]^-$.

Equilibrium 1 is slow with a forward rate of 4.56×10^{-4} and $4.06 \times 10^{-4} \text{ s}^{-1}$ for $\text{LL} = \text{bipy}$ and phen respectively at 0.01 mol dm^{-3} and ionic strength of 0.10 mol dm^{-3} . The specific rate constant for the initial decrease in absorbance (k_4) represents the outer-sphere electron transfer involving the protonated cobalt complex. The specific rate constant (k_5) for the subsequent increase in absorbance corresponds to the formation of the azido-bridged binuclear intermediate (ISC) in step 4, and the specific rate constant for the final decrease in absorbance (k_5) represents the electron transfer following the formation of the bridged intermediate. These rate parameters are indicated in Table 2. The proposed structure for the ISC is

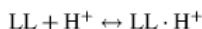


Azide has been shown to be a good bridging ligand in some previously reported electron-transfer studies [29, 30].

Davies and Espenson [31] reported that $\text{Co}(\text{CN})_5 \text{N}_3^{3-}$ reacts with V(II) via an inner-sphere mechanism in the presence of acid. The intermediate in that case could not be isolated due to the fact that the Co(III) complex was in large excess in the reaction systems. The same condition obtains in the present study due to the low extinction coefficient of the cobalt complex. These observations further support reaction step (4) as accounting for the initial decrease in absorbance observed in Figs. 2 and 3 while step (3) is responsible for the increase in absorbance that follows the formation of an inner-sphere complex with an azido bringing ligand. Additional evidence for the above mechanism comes from the addition of phenanthroline which is observed to inhibit the reaction in agreement with the proposed rate law. We did not observe N_3^- attached to Fe in the final product. We suspect that this species may be highly labile in acid.

One would expect that the symmetry of N_3^- as a bridging ligand in $[(\text{HCN})_2(\text{CN})_3\text{CoN-N-N} \cdots \text{Fe}(\text{LL})_2(\text{H}_2\text{O})]^+$ should make $\text{Co}(\text{HCN})_2(\text{CN})_3\text{N}_3^-$ a more efficient oxidant over the outer-sphere counterpart $[\text{Co}(\text{HCN})_2(\text{CN})_3\text{N}_3^-, \text{Fe}(\text{LL})_3^{2+}]$. However, our data shows that the electron transfer is more efficient in the latter, perhaps, due to electron tunnelling via the solvent molecules.

The forward reaction in step 3, characterized by k_c , is catalysed by acid. The concentration of ISC increases with acid due to the protonation of the ligand LL which further drives the equilibrium 1 to the right via



and hence makes more of the dissociated Fe(II) complex available for azide bridging. The protonation of both bipyridine and phenanthroline is well established in the literature [21] and has been proposed as an explanation for the lability of $\text{Fe}(\text{LL})_3^{2+}$ in acid.

At high acid concentration, there is more reaction through ISC since the concentration of this intermediate becomes higher with increasing $[\text{H}^+]$ (Fig. 2). From the rate law,

$$k_{\text{obs}} = \frac{[k_4 K_p [\text{LL}] + k_5 K_{\text{ISC}} K_d] [\text{Co}] [\text{H}^+]^2}{[\text{LL}] + K_d + K_{\text{ISC}} K_p K_d [\text{Co}] [\text{H}^+]^2}$$

Under this condition,

$$K_{\text{ISC}} K_p K_d [\text{Co}] [\text{H}^+]^2 \gg [\text{LL}] + K_d$$

$$\text{and } k_5 K_{\text{ISC}} K_d \gg k_4 K_p [\text{LL}]$$

Hence, the limit $k_{\text{obs}} = k_5$ at high acid concentration indicating the reaction is essentially through the inner-sphere pathway.

The reaction of the ISC is a unimolecular process involving intramolecular electron transfer and should therefore be independent of acid, in agreement with the

observed data (Table 2), where k_5 is approximately $1.540 \times 10^{-4} \text{ s}^{-1}$ for bipy and $1.103 \times 10^{-4} \text{ s}^{-1}$ for phen. On the other hand, reaction step 4 is bimolecular and dependent on the protonation of the cobalt complex in step 2. Hence, k_4 should be significantly acid dependent again in agreement with the experimental data which show that k_4 increases with $[\text{H}^+]$. The higher reactivity of the protonated cobalt complex is in conformity with our study on similar systems [7, 32]. The constant k_c is the forward rate constant for Eq. 3 for the formation of ISC. The formation of ISC is catalysed through shifting equilibrium (1) to the right by removing the dissociated ligand (LL) as shown above. k_c is acid dependent, in agreement with the observed data. The bulkier $\text{Fe}(\text{phen})_3^{2+}$ complex means that the distance of closest approach before electron transfer will be longer than that for $\text{Fe}(\text{bipy})_3^{2+}$. This steric factor ensures higher k_5 values for the electron-transfer reaction of the latter. The same effect is observed in neutral medium as indicated earlier.

Acknowledgement The authors wish to acknowledge the Organisation for the Prohibition of Chemical Weapons (OPCW) for the fund granted to carry out this research work at the University of Botswana, Gaborone, Botswana.

References

1. Adaikalasamy KJ, Venkataramanan NS, Rajagopal S (2003) *Tetrahedron* 59(20):3613. doi:10.1016/S0040-4020(03)00509-X
2. Scholten U, Castillejo A, Bemaner K (2005) *J R Soc Interface* 2(2):109. doi:10.1098/rsif.2004.0023
3. Muresanu L, Pristovsek P, Löhr F, Maneg O, Mukrasch DM, Rüterjans H, Ludwig B, Lücke C (2006) *J Biol Chem* 281(20):14503. doi:10.1074/jbc.M601108200
4. Du G, Espenson JH (2006) *Inorg Chem* 45(3):1053. doi:10.1021/ic0511524
5. Hu D, Lu P (2006) In: *Molecule detection technology proceedings of the SPIE*, vol 42, pp 6092
6. Ojo JF, Ige J, Ogunlusi GO, Owoyomi OO, Olaneni SE (2005) *Trans Met Chem* 31:337. doi:10.1007/s11243-005-6398-8
7. Ojo JF, Ige J, Ogunlusi GO, Owoyomi O, Olaneni ES (2006) *Trans Met Chem* 31:782. doi:10.1007/s11243-006-0073-6
8. Adegite A, Dusumu M, Ojo JF (1977) *J Chem Soc (Dalton Trans)* 630
9. Ige J, Nnadi R, Ojo JF, Olubuyide O (1978) *J Chem Soc (Dalton Trans)* 148
10. Baxendale JH, Fielden EM, Keene JP (1965) *Proc R Soc Lond A Math Phys Sci* 286:320
11. Castellano EE, Piro OE, Punte G, Amalvy JI, Varetto EL, Aymonino PJ (1982) *Acta Cryst B* 38:2239. doi:10.1107/S0567740882008401
12. Piro OE (1985) *Phys Rev B* 31:1122. doi:10.1103/PhysRevB.31.1122
13. Adegboro AB, Ojo JF, Olubuyide O, Sheyin OT (1987) *Inorg Chim Acta* 131:247. doi:10.1016/S0020-1693(00)96033-X
14. Oyetunji O, Olubuyide O, Ojo JF (1990) *Bull Chem Soc Jpn* 63:601. doi:10.1246/bcsj.63.601

15. Shakhshiri BZ, Gordon G (1968) *Inorg Chem* 7:2454. doi: [10.1021/ic50069a055](https://doi.org/10.1021/ic50069a055)
16. Przystas TJ, Sutin N (1973) *J Am Chem Soc* 95:5545. doi: [10.1021/ja00798a020](https://doi.org/10.1021/ja00798a020)
17. Grassi R, Haim R, Wilmarth WK (1962) *Inorg Chem* 6:237. doi: [10.1021/ic50048a010](https://doi.org/10.1021/ic50048a010)
18. Flor T, Casabo J (1986) *Synth React Inorg Met Org Chem* 16(6):795. doi: [10.1080/00945718608071359](https://doi.org/10.1080/00945718608071359)
19. Espenson JH (1965) *Inorg Chem* 4:121. doi: [10.1021/ic50023a032](https://doi.org/10.1021/ic50023a032)
20. Lappin AG (1994) *Redox mechanisms in inorganic organic chemistry*. Ellis Horwood, Chichester, p 118
21. Tobe ML, Burgess J (1999) *Inorganic reaction mechanism*. Addison Wesley Longman Limited, USA, p 424
22. Rodriguez A, Graciani M, Balahura R, Moya ML (1996) *J Phys Chem* 100:16978. doi: [10.1021/jp961175r](https://doi.org/10.1021/jp961175r)
23. Ukoha PO, Iyun JF (2001) *J Chem Soc Niger* 26(2):163
24. Ukoha PO, Iyun JF (2002) *J Chem Soc Niger* 27:119
25. Jenkins IL, Monk CB (1951) *J Chem Soc* 68. doi: [10.1039/jr9510000068](https://doi.org/10.1039/jr9510000068)
26. Ali K, Ashiq U (2004) *J Iran Soc* 1(2):122
27. Staples PJ (1971) *J Chem Soc A* 2213. doi: [10.1039/j19710002213](https://doi.org/10.1039/j19710002213)
28. Ige J, Ojo JF, Olubuyide O (1980) *Inorg Chem* 20:1757. doi: [10.1021/ic50220a029](https://doi.org/10.1021/ic50220a029)
29. Haim A (1983) *Prog Inorg Chem* 30:273. doi: [10.1002/9780470166314.ch6](https://doi.org/10.1002/9780470166314.ch6)
30. Ribas J, Escuer A, Monfort M, Vicente R, Cortés R, Lezama L, Rojo T (1999) *Coord Chem Rev* 1027. doi: [10.1016/S0010-8545\(99\)00051-X](https://doi.org/10.1016/S0010-8545(99)00051-X)
31. Davies KM, Espenson JH (1969) *J Am Chem Soc* 3093. doi: [10.1021/ja01039a049](https://doi.org/10.1021/ja01039a049)